







Communication

# Estimating Summer Arctic Warming Amplitude Relative to Pre-Industrial Levels Using Tree Rings

Cong Gao <sup>1,2</sup>, Chunming Shi <sup>1,\*</sup> , Yuxin Lou <sup>1</sup>, Ran An <sup>1</sup>, Cheng Sun <sup>1</sup> , Guocan Wu <sup>1</sup> , Yuandong Zhang <sup>3</sup> , Miaogen Shen <sup>4</sup>  and Deliang Chen <sup>5</sup> 

- <sup>1</sup> College of Global Change and Earth System Science, Beijing Normal University, Beijing 100875, China  
<sup>2</sup> Department of Geography, University of Hong Kong, Hong Kong 999077, China  
<sup>3</sup> Key Laboratory of Forest Ecology and Environment of National Forestry and Grassland Administration, Research Institute of Forest Ecology, Environment and Protection, Chinese Academy of Forestry, Beijing 100091, China  
<sup>4</sup> State Key Laboratory of Earth Surface Processes and Resource Ecology, Faculty of Geographical Science, Beijing Normal University, Beijing 100875, China  
<sup>5</sup> Regional Climate Group, Department of Earth Sciences, University of Gothenburg, 40530 Gothenburg, Sweden  
\* Correspondence: chunming.shi@gmail.com

**Abstract:** Estimating long-term trends and short-term amplitudes requires reliable temperature (Temp) observations in the pre-industrial period when few in situ observations existed in the Arctic. Tree-ring materials are most available and used to reconstruct past Arctic Temp variations. However, most previous studies incorporated materials that are insensitive to local Temp variabilities. The derived reconstruction qualities are low (indicated by low calibration  $R^2$ ), and the uncertainties inherent in the various detrending methodologies are unknown. To reconstruct Arctic (N60°–N90°) summer (June–August) Temp in 1850–1900 and variations over the past centuries, we screened 1116 tree-ring width and tree-ring density records and applied four detrending functions (sf-RCS, RCS, MOD, and spline). In total, 338–396 records show significant correlations ( $p < 0.05$ ) with the Climate Research Unit (CRU) Temp of the corresponding grid point. These records were selected and combined into a proxy record. The achieved Arctic summer Temp reconstruction explained 45–57% of the instrumental summer Temp variance since 1950. The 2012–2021 summer Arctic warming amplitudes (1.42–1.74 °C) estimated by Temp anomaly datasets extending back to 1850 are within the range derived from our reconstructions, despite using various detrending methods. These findings could suggest the Berkeley and HadCRU5 datasets interpolating Temp from a few (6–73) meteorological stations could still represent the mean Arctic Temp variation in 1850–1900, and the updated reconstruction can be used as a reliable reference for 1550–2007 Arctic summer Temp history.

**Keywords:** arctic; climate change; tree ring



**Citation:** Gao, C.; Shi, C.; Lou, Y.; An, R.; Sun, C.; Wu, G.; Zhang, Y.; Shen, M.; Chen, D. Estimating Summer Arctic Warming Amplitude Relative to Pre-Industrial Levels Using Tree Rings. *Forests* **2023**, *14*, 418. <https://doi.org/10.3390/f14020418>

Academic Editor: Giovanni Leonelli

Received: 12 January 2023

Revised: 5 February 2023

Accepted: 14 February 2023

Published: 17 February 2023



**Copyright:** © 2023 by the authors. Licensee MDPI, Basel, Switzerland. This article is an open access article distributed under the terms and conditions of the Creative Commons Attribution (CC BY) license (<https://creativecommons.org/licenses/by/4.0/>).

## 1. Introduction

With a warming rate two to four times the global mean, global climate change most strongly affects the Arctic [1,2]. In addition to the greenhouse gas increase, “Arctic amplification” was attributed to positive albedo feedbacks including but not limited to snow cover melting, Arctic Ocean ice extent reduction, snowless season lengthening, and increased vegetation–atmosphere–sea ice interaction [3–6]. The rapid Arctic warming has led to extensive environmental impacts, such as permafrost thawing, mountain glaciers and the Greenland ice sheet melting, and more frequent boreal forest wildfires [7–9]. All these changes are most pronounced in the summer, allowing for the additional release of greenhouse gases and albedo decrease, which have in turn aggravated the summer heatwaves in northern high latitudes [10,11], contributed to global warming [7,12], and significantly affected sustainable development [13].

Given the inherent higher warming rates over global land than the ocean and for the high-latitude land surface than the low-latitude land surface, a certain amount of global mean temperature (Temp) increase corresponds to much larger warming amplitudes over the terrestrial northern pole region [13]. Understanding the Arctic's climate history and correctly estimating warming amplitude are crucial for predicting future climate states and their impacts. However, these goals are difficult to achieve due to the sparse and short in situ observations in the Arctic, especially during the early stage. The IPCC 1.5 °C special report has shown that the current Arctic warming relative to 1850–1900 (defined as the pre-industrial) is higher than 2 °C for the annual mean and above 3 °C for the winter [13]. However, only a few instrumental data exist in the Arctic during that period.

Tree-ring records are a reliable proxy of past climate variability and are widely distributed in Arctic forests. The low thermal availability of the growing season limited the radial growth of boreal forests, making them potentially useful for reconstructing summer temperatures. The existing Arctic Temp reconstructions exhibit low temporal resolutions [14,15], are based on poor geographic coverage [14–16], incorporate proxies originally targeting the Temp of varying seasons [16–18], or use calibrations conducted within periods when extensive in situ observations are scarce [16,18,19]. This study collected all available tree-ring width and density data over the entire terrestrial Arctic, covering many more sites than previous studies. The age-related signals inherent in tree-ring measurements were removed using four functions to estimate the method-derived errors, and only the records showing significant correlations with local summer Temp within the corresponding grid points were used to achieve an annual-resolved reconstruction. The calibration was conducted in the post-1950 period when the instrumental observations are reliable, and the reconstruction quality was shown to be higher than in previous studies.

## 2. Data and Methods

### 2.1. Temperature, Tree Ring, and Meteorological Station Information

The land surface Temp was obtained from the Climate Research Unit Timeseries (CRU TS) 4.06 dataset [20], and a 1901–2021 monthly  $0.5^\circ \times 0.5^\circ$  gridded interpolation of instrumental observations was used as the reconstruction target; monthly Temp anomaly datasets with lower resolutions, including 1768–2021  $1^\circ \times 1^\circ$  land-surface Berkeley [21] and 1850–2021  $5^\circ \times 5^\circ$  HadCRUT5, were obtained [22], and land surface data in the Arctic (N60°–N90°) were extracted. For HadCRUT5, only the grid points covering more than 50% of the land were used.

Tree-ring width and density measurements of 1116 sites within N60°–N90° were collected from the International Tree Ring Data Bank. The age-related growth trend was removed using four detrending methods, including signal-free regional curve standardization (sf-RCS) [23], regional curve standardization (RCS) [24], 67% spline [25], and the modified negative exponential curve (MOD) [26], to estimate the inherent reconstruction error. The detrended data were standardized into four tree-ring records for each site. Conservative detrending such as spline and MOD can remove age-related and long-term climatic signals, but they were frequently used in previous tree-ring width-based climate reconstructions. RCS can avoid the frequency limitation of the curve fitting process. On its basis, sf-RCS can preserve long-term climatic signals and avoids end-effect distortion [27].

More than 2000 meteorological stations in the Arctic region were collected from the Global Historical Climatology Network Daily Database (GHCNd) [28], Environment and Climate Change Canada [29], and All-Russia Institute of Hydrometeorological Information—World Data Centre [28]. Detailed information on the meteorological stations includes latitude, longitude, observation elements, and start and end year. Early-stage Temp observations are sparse and less representative in the Arctic, with only 78 stations with data before 1900 (Figure 1). The detailed information on these stations is presented in Table S1. The number of tree-ring sites is much larger and more widely distributed than those of the stations in the Arctic (Figure 1).

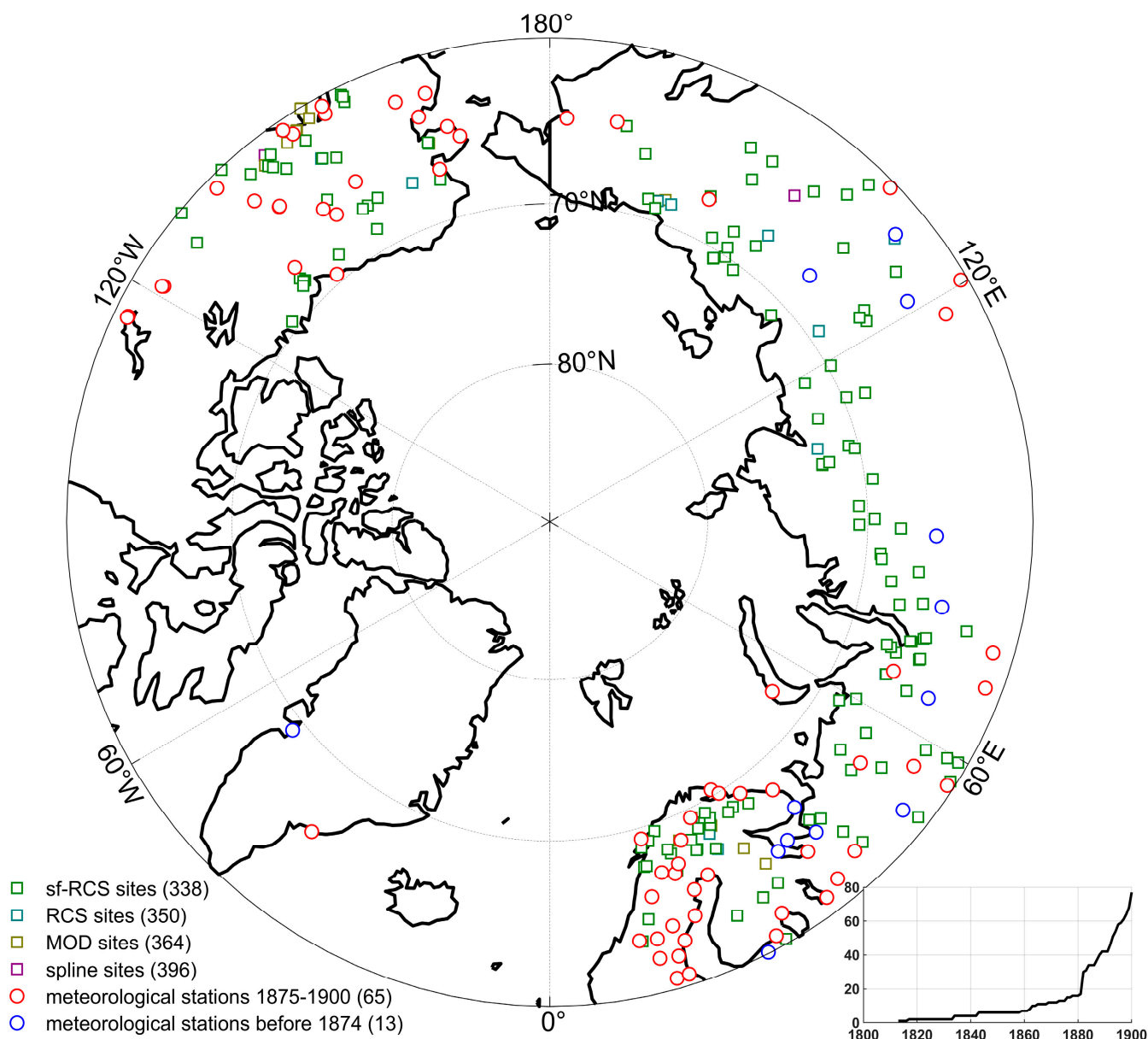


**Figure 1.** The green, blue, yellow, and purple squares show sites with tree-ring width and density records showing significant ( $p < 0.05$ ) correlations with the CRU summer Temp of the corresponding grid point with sf-RCS, RCS, MOD, and spline detrending methods, respectively. The red and blue circles indicate the meteorological stations with Temp between 1875 and 1900 and before 1874 in the Arctic, respectively. The insert at the right bottom shows the number of meteorological stations from 1800 to 1900 in the Arctic.

Among the existing Arctic Temp anomaly reconstructions [14–19,30], the ones targeting the summer season were downloaded from the National Oceanic and Atmospheric Administration (NOAA) paleoclimate database [14,16,19].

## 2.2. Reconstruction

The CRU summer (June–August, JJA) Temp records for each tree-ring width and density site were extracted from the corresponding grid point. The detrend and standardized tree-ring width and density records showing a significant positive correlation ( $p < 0.05$ ) with the summer Temp of the corresponding grid point within the maximum overlapping periods since 1950 (at least 30 years) are selected for reconstruction. All the chosen tree-

ring width and density records developed by the same detrending method were Z-score normalized and then averaged into a single Arctic Temp proxy record.

A linear regression model between the Arctic Temp proxy record and the regional mean Arctic (N60°–N90°) CRU summer Temp was developed and used for the reconstruction. The CRU Temp before 1950 was not used to ensure data and calibration qualities because they were interpolations of distant meteorological stations. All reconstructions were smoothed by the 30-year LOESS (locally weighted smoothing) method to show the multi-decadal variability [31]. The 2012–2021 CRU mean values, representing the current Arctic summer Temp, were subtracted by the 1850–1900 means of CRU reconstructions to calculate the warming amplitudes above the pre-industrial level. The obtained results were compared with the same warming amplitudes for Berkeley and HadCRUT5 themselves.

The reconstruction errors were calculated as follows: The Arctic CRU summer Temp and the Arctic tree-ring record were randomly split into two halves within the calibration period of 1950–2007. Each half was used to establish a linear calibration model and validated with the other half, yielding 57 error values (the difference between target data and calibration model prediction). This process was repeated 1000 times. The 2.5% and 97.5% percentiles of the total error distribution were defined as the 95% confidence interval of the reconstruction.

### 3. Results

Tree-ring records showing significant correlations with the CRU summer mean Temp of the corresponding grid point were obtained, which extended from Scandinavia to eastern Siberia of the Eurasian Continent, and they were also found over Alaska and Northwest Canada. No data were obtained in the tree-less regions, such as the glaciers of Northeast Canada and the Greenland ice sheet (Figure 1). The number of chosen records was 338 for sf-RCS, 350 for RCS, 364 for MOD, and 396 for Spline (Table S2).

Among the meteorological stations in the Arctic, there are only 6–73 with mean, maximum, or minimum Temp data within 1850–1900 (Figure 1), which are sparsely distributed in West and Northwest Europe and Canada. Early-stage Temp observations numbered much fewer in Siberia and Greenland.

We developed four Arctic land-surface summer Temp reconstructions spanning 1550–2007 using sf-RCS, RCS, MOD, and spline detrending methods with high calibration qualities (indicated by  $R^2$ ), which explained the 55%, 57%, 52%, and 45% variabilities of the CRU data during 1950–2007, respectively (all  $p < 0.001$ , Figure 2a–d), with the 95% confidence intervals of  $\pm 0.63$  °C,  $\pm 0.59$  °C,  $\pm 0.64$  °C, and  $\pm 0.69$  °C, respectively. The warming trends of our reconstruction are comparable with those of the CRU datasets during 1950–2007. The warming amplitude of 2012–2021 CRU summer Temp reached  $1.21 \pm 0.63$  °C,  $1.26 \pm 0.59$  °C,  $1.11 \pm 0.64$  °C, and  $0.95 \pm 0.69$  °C above the 1850–1900 reconstruction mean (red dashed line in Figure 2a–d), respectively. The reconstructed and instrumental summer Arctic Temp showed close coherence since the 1900s (Figure 2e). While our reconstructions are relatively stable in the 1850s–1900s, the instrumental data show decreasing trends (Figure 2e).

The 2012–2021 instrumental Arctic land (Berkeley and HadCRUT5) summer Temp anomalies have warmed 1.42 and 1.74 °C above their pre-industrial levels, which are both within the range of our estimations for CRU reconstructions (between  $0.95 \pm 0.67$  and  $1.26 \pm 0.59$  °C in Figure 2).

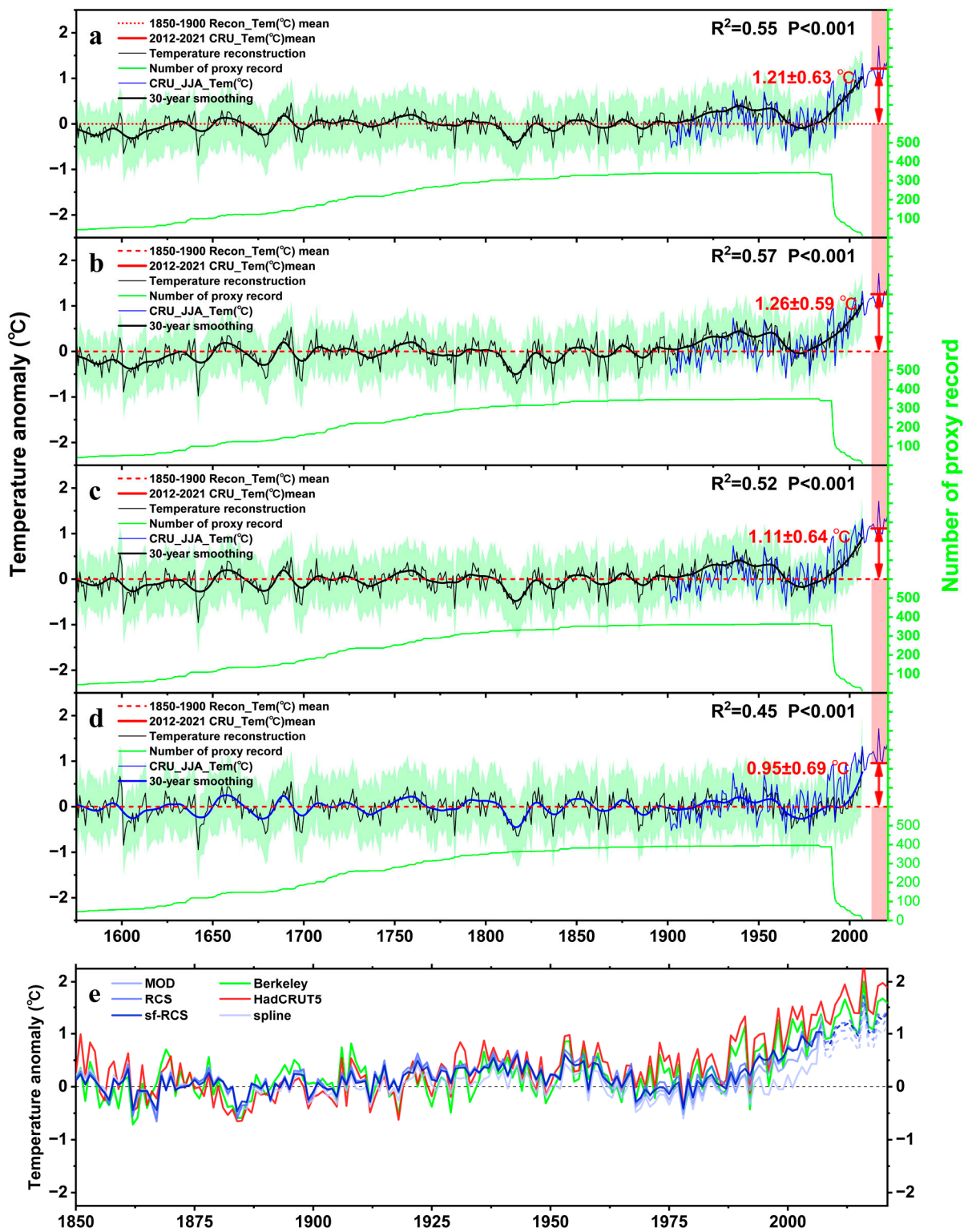


**Figure 2.** (a) Instrumental (CRU TS 4.06, blue line) and reconstructed (thin black line) Arctic summer Temp using sf-RCS detrending. Green shading is the 95% confidence interval. The green line is the number of tree-ring records combined for reconstruction, and the thick black line is the 30-year LOESS smoothing. The red dotted and thick red horizontal lines represent the mean values of the 1850–1900 reconstruction and 2012–2021 CRU summer Temp; the difference between the two values, represented by the summer Arctic warming amplitude, is denoted with transparent red bars and arrows. (b–d) The same as a but for reconstructions using RCS, MOD, and spline detrending. (e) Summer Temp anomalies relative to 1850–1900 for our reconstruction and instrumental Temp datasets.

#### 4. Conclusions and Discussion

The “Arctic amplification” phenomenon was already identified in the instrumental data in the last decades and substantially contributed to the global warming trend [12]. However, the scarcity of early meteorological stations with poor spatial coverage has inevitably led to biased Temp observations in the Arctic during the pre-industrial period. With a much larger site number and more extensive distribution (338–396 proxy records relative to 6–73 instrumental stations), tree-ring-based Arctic Temp reconstructions are potentially more reliable than Temp datasets in the pre-industrial period. Compared to conservative detrending, including spline and MOD methods, the reconstructions developed by RCS and sf-RCS exhibit higher calibration quality ( $R^2 = 0.57$  and  $0.55$ , relative to  $R^2 = 0.45$  and  $0.52$ ) and larger warming amplitudes in 2012–2021 ( $1.26 \pm 0.59$  °C and  $1.21 \pm 0.63$  °C relative to  $0.95 \pm 0.67$  °C and  $1.11 \pm 0.64$  °C above their pre-industrial level). Studies have shown that RCS is superior for the retention of low-frequency trends compared to traditional detrending methods (spline and MOD) [32]. Tree-ring based reconstructions well coincide with the instrumental datasets (Berkeley and HadCRUT5) in 1850–1970. However, since the mid-1980s, all reconstructions have shown negative anomalies compared to the instrumental data. The possible underestimations of the reconstructions could arise from the “divergence problem” [33] or from removing too much long-term variability inherent in traditional detrending methods. Meanwhile, the rapid Arctic meteorological station increase since the 1950s may explain the difference between reconstructions and instrumental datasets as well [34].

The instrumental Arctic land (Berkeley and HadCRUT5) datasets reported warming amplitudes (1.42 and 1.74 °C, respectively) in the last decade relative to pre-industrial levels. The possible overestimation is likely due to the discrepancy of Temp in our reconstructions and Temp anomaly datasets within 1850–1900, when extensive in situ observations did not exist, and instrumental Temp datasets are actually interpolations of remote observations. The bias was further aggravated by using equal-angle grids in CRU, HadCRU, and Berkeley datasets [35]. Moreover, some early land surface Temp data were derived from sea surface Temp, which in turn led to more biases [36]. Despite the bias, the constant temperature increase was evident for all instrumental datasets and all reconstructions. The warming amplitudes derived from temperature anomaly datasets (1.42 and 1.74 °C) are within the range derived from our reconstructions. However, we still believe that our reconstruction should be carefully used.

Previous Arctic summer Temp anomaly reconstructions were obtained and compared to the anomalies of our reconstructions relative to 1850–1900 (Figure S1). Some previous reconstructions have shown lower or higher warming amplitudes [16,19]. However, the number of proxy records and calibration  $R^2$  is much smaller, thus resulting in much larger reconstruction uncertainty. The resolutions of some reconstructions were 5- and 10-year [14,15], and the rest were reconstructions of Arctic land–ocean Temp [15,17,30]. With higher calibration qualities and resolutions, our updated reconstructions can be used as a reference of past Arctic land temperature history spanning 1550–2007.

**Supplementary Materials:** The following supporting information can be downloaded at <https://www.mdpi.com/article/10.3390/f14020418/s1>. Table S1: The meteorological stations we collected before 1900; Table S2: The site names of tree rings used for summer Arctic temperature reconstructions; Figure S1: Arctic summer temperature anomalies relative to 1850–1900 for previous reconstructions and our reconstructions.

**Author Contributions:** Conceptualization, C.S. (Chunming Shi); methodology, C.S. (Chunming Shi); software, C.G.; validation, C.S. (Chunming Shi) and C.G.; formal analysis, C.G.; investigation, C.G.; resources, R.A.; data curation, C.G.; writing—original draft preparation, C.S. (Chunming Shi) and C.G.; writing—review and editing, Y.L., C.S. (Cheng Sun), G.W., Y.Z., M.S. and D.C.; visualization, C.G.; supervision, C.S. (Chunming Shi); project administration, C.S. (Chunming Shi); funding acquisition, C.S. (Chunming Shi) All authors have read and agreed to the published version of the manuscript.

**Funding:** This research was funded by the National Natural Science Foundation of China, 31971667.

**Data Availability Statement:** Publicly available datasets were analyzed in this study. These data can be found here: tree-ring width and density records and previous reconstructions (<https://www.ncei.noaa.gov/products/paleoclimatology/>, accessed on 21 May 2022); Climate Research Unit (<https://crudata.uea.ac.uk/cru/data/hrg/>, accessed on 21 May 2022); Berkeley (<https://berkeleyearth.org/data/>, accessed on 21 May 2022); HadCRUT5 (<https://www.metoffice.gov.uk/hadobs/hadcrut5/>, accessed on 21 May 2022); Global Historical Climatology Network - Daily Database (<https://www.ncei.noaa.gov/products/land-based-station/global-historical-climatology-network-daily>, accessed on 24 September 2022).

**Conflicts of Interest:** The authors declare no conflict of interest.

## References

1. Graversen, R.G.; Mauritsen, T.; Tjernstrom, M.; Kallen, E.; Svensson, G. Vertical Structure of Recent Arctic Warming. *Nature* **2008**, *451*, 53–56. [[CrossRef](#)]
2. Screen, J.A.; Deser, C.; Simmonds, I. Local and Remote Controls on Observed Arctic Warming. *Geophys. Res. Lett.* **2012**, *39*, L10709. [[CrossRef](#)]
3. Chapin, F.S.; Sturm, M.; Serreze, M.C.; McFadden, J.P.; Key, J.R.; Lloyd, A.H.; McGuire, A.D.; Rupp, T.S.; Lynch, A.H.; Schimel, J.P.; et al. Role of Land-Surface Changes in Arctic Summer Warming. *Science* **2005**, *310*, 657–660. [[CrossRef](#)] [[PubMed](#)]
4. Serreze, M.C.; Barrett, A.P.; Stroeve, J.C.; Kindig, D.N.; Holland, M.M. The Emergence of Surface-Based Arctic Amplification. *Cryosphere* **2009**, *3*, 11–19. [[CrossRef](#)]
5. Wunderling, N.; Willeit, M.; Donges, J.F.; Winkelmann, R. Global Warming Due to Loss of Large Ice Masses and Arctic Summer Sea Ice. *Nat. Commun.* **2020**, *11*, 5177. [[CrossRef](#)]
6. Jeong, J.-H.; Kug, J.-S.; Linderholm, H.W.; Chen, D.; Kim, B.-M.; Jun, S.-Y. Intensified Arctic Warming under Greenhouse Warming by Vegetation-Atmosphere-Sea Ice Interaction. *Environ. Res. Lett.* **2014**, *9*, 094007. [[CrossRef](#)]
7. Shepherd, T.G. Effects of a Warming Arctic. *Science* **2016**, *353*, 989–990. [[CrossRef](#)] [[PubMed](#)]
8. Stieglitz, M.; Dery, S.J.; Romanovsky, V.E.; Osterkamp, T.E. The Role of Snow Cover in the Warming of Arctic Permafrost. *Geophys. Res. Lett.* **2003**, *30*, 1721. [[CrossRef](#)]
9. Walker, X.J.; Baltzer, J.L.; Cumming, S.G.; Day, N.J.; Ebert, C.; Goetz, S.; Johnstone, J.F.; Potter, S.; Rogers, B.M.; Schuur, E.A.G.; et al. Increasing Wildfires Threaten Historic Carbon Sink of Boreal Forest Soils. *Nature* **2019**, *572*, 520–523. [[CrossRef](#)] [[PubMed](#)]
10. Fischer, E.M.; Schaer, C. Consistent Geographical Patterns of Changes in High-Impact European Heatwaves. *Nat. Geosci.* **2010**, *3*, 398–403. [[CrossRef](#)]
11. Hu, S.; Zhang, L.; Qian, S. Marine Heatwaves in the Arctic Region: Variation in Different Ice Covers. *Geophys. Res. Lett.* **2020**, *47*, e2020GL089329. [[CrossRef](#)]
12. Huang, J.; Zhang, X.; Zhang, Q.; Lin, Y.; Hao, M.; Luo, Y.; Zhao, Z.; Yao, Y.; Chen, X.; Wang, L.; et al. Recently Amplified Arctic Warming Has Contributed to a Continual Global Warming Trend. *Nat. Clim. Chang.* **2017**, *7*, 875–879. [[CrossRef](#)]
13. IPCC. *Global Warming of 1.5 °C: IPCC Special Report on Impacts of Global Warming of 1.5 °C above Pre-Industrial Levels in Context of Strengthening Response to Climate Change, Sustainable Development, and Efforts to Eradicate Poverty*; Cambridge University Press: Cambridge, UK, 2022.
14. Kaufman, D.S.; Schneider, D.P.; McKay, N.P.; Ammann, C.M.; Bradley, R.S.; Briffa, K.R.; Miller, G.H.; Otto-Bliesner, B.L.; Overpeck, J.T.; Vinther, B.M. Recent Warming Reverses Long-Term Arctic Cooling. *Science* **2009**, *325*, 1236–1239. [[CrossRef](#)]
15. Overpeck, J.; Hughen, K.; Hardy, D.; Bradley, R.; Case, R.; Douglas, M.; Finney, B.; Gajewski, K.; Jacoby, G.; Jennings, A.; et al. Arctic Environmental Change of the Last Four Centuries. *Science* **1997**, *278*, 1251–1256. [[CrossRef](#)]
16. Shi, F.; Yang, B.; Ljungqvist, F.C.; Yang, F. Multi-Proxy Reconstruction of Arctic Summer Temperatures over the Past 1400 Years. *Clim. Res.* **2012**, *54*, 113–128. [[CrossRef](#)]
17. McKay, N.P.; Kaufman, D.S. An Extended Arctic Proxy Temperature Database for the Past 2000 Years. *Sci. Data* **2014**, *1*, 140026. [[CrossRef](#)]
18. Ahmed, M.; Anchukaitis, K.J.; Asrat, A.; Borgaonkar, H.P.; Braida, M.; Buckley, B.M.; Buntgen, U.; Chase, B.M.; Christie, D.A.; Cook, E.R.; et al. Continental-Scale Temperature Variability during the Past Two Millennia. *Nat. Geosci.* **2013**, *6*, 339–346. [[CrossRef](#)]
19. Werner, J.P.; Divine, D.V.; Ljungqvist, F.C.; Nilsen, T.; Francus, P. Spatio-Temporal Variability of Arctic Summer Temperatures over the Past 2 Millennia. *Clim. Past.* **2018**, *14*, 527–557. [[CrossRef](#)]
20. Harris, I.; Osborn, T.J.; Jones, P.; Lister, D. Version 4 of the CRU TS Monthly High-Resolution Gridded Multivariate Climate Dataset. *Sci. Data* **2020**, *7*, 109. [[CrossRef](#)]
21. Rohde, R.A.; Hausfather, Z. The Berkeley Earth Land/Ocean Temperature Record. *Earth Syst. Sci. Data* **2020**, *12*, 3469–3479. [[CrossRef](#)]

22. Morice, C.P.; Kennedy, J.J.; Rayner, N.A.; Winn, J.P.; Hogan, E.; Killick, R.E.; Dunn, R.J.H.; Osborn, T.J.; Jones, P.D.; Simpson, I.R. An Updated Assessment of Near-Surface Temperature Change From 1850: The HadCRUT5 Data Set. *J. Geophys. Res. Atmos.* **2021**, *126*, e2019JD032361. [[CrossRef](#)]
23. Melvin, T.M.; Briffa, K.R. A “Signal-Free” Approach to Dendroclimatic Standardisation. *Dendrochronologia* **2008**, *26*, 71–86. [[CrossRef](#)]
24. Briffa, K.; Jones, P.; Bartholin, T.; Eckstein, D.; Schweingruber, F.; Karlen, W.; Zetterberg, P.; Eronen, M. Fennoscandian Summers from Ad-500—Temperature-Changes on Short and Long Timescales. *Clim. Dyn.* **1992**, *7*, 111–119. [[CrossRef](#)]
25. Briffa, K.R.; Osborn, T.J.; Schweingruber, F.H.; Harris, I.C.; Jones, P.D.; Shiyatov, S.G.; Vaganov, E.A. Low-Frequency Temperature Variations from a Northern Tree Ring Density Network. *J. Geophys. Res.-Atmos.* **2001**, *106*, 2929–2941. [[CrossRef](#)]
26. Cook, E.; Briffa, K.; Meko, D.; Graybill, D.; Funkhouser, G. The Segment Length Curse in Long Tree-Ring Chronology Development for Paleoclimatic Studies. *Holocene* **1995**, *5*, 229–237. [[CrossRef](#)]
27. Melvin, T.M.; Briffa, K.R. CRUST: Software for the Implementation of Regional Chronology Standardisation: Part 1. Signal-Free RCS. *Dendrochronologia* **2014**, *32*, 7–20. [[CrossRef](#)]
28. Menne, M.J.; Durre, I.; Vose, R.S.; Gleason, B.E.; Houston, T.G. An Overview of the Global Historical Climatology Network-Daily Database. *J. Atmos. Ocean. Technol.* **2012**, *29*, 897–910. [[CrossRef](#)]
29. Vincent, L.A.; Wang, X.L.; Milewska, E.J.; Wan, H.; Yang, F.; Swail, V. A Second Generation of Homogenized Canadian Monthly Surface Air Temperature for Climate Trend Analysis. *J. Geophys. Res. Atmos.* **2012**, *117*, D18110. [[CrossRef](#)]
30. Shi, F.; Duan, A.; Yin, Q.; Bruun, J.T.; Xiao, C.; Guo, Z. Modulation of the Relationship between Summer Temperatures in the Qinghai–Tibetan Plateau and Arctic over the Past Millennium by External Forcings. *Quat. Res.* **2021**, *103*, 130–138. [[CrossRef](#)]
31. Shi, C.; Daux, V.; Li, Z.; Wu, X.; Fan, T.; Ma, Q.; Wu, X.; Tian, H.; Carré, M.; Ji, D.; et al. The Response of Relative Humidity to Centennial-Scale Warming over the Southeastern Tibetan Plateau Inferred from Tree-Ring Width Chronologies. *Clim. Dyn.* **2018**, *51*, 3735–3746. [[CrossRef](#)]
32. D’Arrigo, R.; Wilson, R.; Jacoby, G. On the Long-Term Context for Late Twentieth Century Warming. *J. Geophys. Res. Atmos.* **2006**, *111*, D03103. [[CrossRef](#)]
33. D’Arrigo, R.; Wilson, R.; Liepert, B.; Cherubini, P. On the ‘Divergence Problem’ in Northern Forests: A Review of the Tree-Ring Evidence and Possible Causes. *Glob. Planet. Chang.* **2008**, *60*, 289–305. [[CrossRef](#)]
34. Bekryaev, R.V.; Polyakov, I.V.; Alexeev, V.A. Role of Polar Amplification in Long-Term Surface Air Temperature Variations and Modern Arctic Warming. *J. Clim.* **2010**, *23*, 3888–3906. [[CrossRef](#)]
35. Cowtan, K.; Way, R.G. Coverage Bias in the HadCRUT4 Temperature Series and Its Impact on Recent Temperature Trends. *Q. J. R. Meteorol. Soc.* **2014**, *140*, 1935–1944. [[CrossRef](#)]
36. Richardson, M.; Cowtan, K.; Hawkins, E.; Stolpe, M.B. Reconciled Climate Response Estimates from Climate Models and the Energy Budget of Earth. *Nat. Clim. Chang.* **2016**, *6*, 931–935. [[CrossRef](#)]

**Disclaimer/Publisher’s Note:** The statements, opinions and data contained in all publications are solely those of the individual author(s) and contributor(s) and not of MDPI and/or the editor(s). MDPI and/or the editor(s) disclaim responsibility for any injury to people or property resulting from any ideas, methods, instructions or products referred to in the content.